N92-14083

Study of Geopotential Error Models Used in Orbit Determination Error Analysis*

C. Yee, D. Kelbel, T. Lee, and M. Samii
COMPUTER SCIENCES CORPORATION (CSC)

G. Mistretta and R. Hart
GODDARD SPACE FLIGHT CENTER (GSFC)

ABSTRACT

The uncertainty in the geopotential model is currently one of the major error sources in the orbit determination of low-altitude Earth-orbiting spacecraft. This paper presents the results of an investigation of different geopotential error models and modeling approaches currently used for operational orbit error analysis support at the Goddard Space Flight Center (GSFC), with emphasis placed on sequential orbit error analysis using a Kalman filtering algorithm.

Several geopotential models, known as the Goddard Earth Models (GEMs), have been developed and used at GSFC for orbit determination. The errors in the geopotential models arise from the truncation errors that result from the omission of higher order terms (omission errors) and the errors in the spherical harmonic coefficients themselves (commission errors). At GSFC, two error modeling approaches have been operationally used to analyze the effects of geopotential uncertainties on the accuracy of spacecraft orbit determination — the *lumped error modeling* and *uncorrelated error modeling*.

The lumped error modeling approach computes the orbit determination errors on the basis of either the calibrated standard deviations of a geopotential model's coefficients or the weighted difference between two independently derived geopotential models. The uncorrelated error modeling approach treats the errors in the individual spherical harmonic components as uncorrelated error sources and computes the aggregate effect using a combination of individual coefficient effects.

The study presented in this paper assesses the reasonableness of the two error modeling approaches in terms of global error distribution characteristics and orbit error analysis results. Specifically, this study presents the global distribution of geopotential acceleration errors for several gravity error models and assesses the orbit determination errors resulting from these error models for three types of spacecraft — the Gamma Ray Observatory, the Ocean Topography Experiment, and the Cosmic Background Explorer.

6130-15

229

1. INTRODUCTION

The Earth's geopotential field, V, is commonly represented by the following spherical harmonic equation:

$$V = \frac{\mu}{r} \left[1 + \sum_{n=2}^{\infty} \sum_{m=0}^{n} (R_e/r)^n \, P_n^m \, (\sin \phi) \, [S_n^m \sin m\lambda + C_n^m \cos m\lambda] \right] \quad (1)$$

where μ = gravitational constant times mass of the Earth

r = spacecraft orbital radius

R_e = radius of the Earth (usually taken as the equatorial radius)

P_n^m = associated Legendre function

S_n^m, C_n^m = harmonic coefficients of degree n and order m

ϕ, λ = geocentric latitude and east longitude

Of computational necessity, the geopotential field represented by Equation (1) is truncated at some finite degree and order. Over the years, several progressively more accurate geopotential models, known as the Goddard Earth Models (GEMs), have been developed and used at Goddard Space Flight Center (GSFC) for satellite orbit determination. Although the geopotential modeling accuracy has improved, it remains one of the major error sources in the orbit determination of low-altitude Earth-orbiting spacecraft. The errors in the geopotential force models arise from the truncation errors resulting from the omission of higher order terms (omission errors) and the errors in the spherical harmonic coefficients (commission errors).

In deriving each GEM, a covariance matrix associated with the spherical harmonic coefficients (or the calibrated form of this matrix) can generally be used to analyze the effects of commission errors on spacecraft orbit determination. However, because of the large size of the matrix, it is computationally expensive and, thus, is impractical for operational use.

As an alternative, a computationally simpler modeling approach, known as the *lumped error model* (Reference 1), has been used at GSFC for orbit error analysis using the batch-weighted least-squares estimation method. A second approach currently being used in sequential error analysis, the *uncorrelated error model*, treats each spherical harmonic component as uncorrelated and considers each to be an independent error source.

1.1 LUMPED ERROR MODEL

In the lumped error modeling approach (LEMA), the orbit determination errors that result from the geopotential model errors are computed by summing algebraically the contributions of the individual spherical harmonic coefficient errors. The algebraic summation assumes that the individual harmonic coefficient errors are fully correlated. This approach also results

in better computational efficiency by having to evaluate only one variational equation to account for the geopotential errors contributed from all harmonic coefficient error sources (Reference 2). The error models used for this approach commonly belong to two categories: *gravity difference* and *standard deviations*.

In the first category, an error model is constructed by taking the weighted difference between two independently derived geopotential model coefficients—the gravity difference error models. The rationale for such an approach is that, if two geopotential models are independently derived, then the weighted average of the two model coefficients may be closer to the "truth," and the weighted difference between the two models can be regarded as a measure of the error for one of the models. However, operationally, the gravity difference models have been usually generated based on differencing two somewhat correlated geopotential models, for example, GEM9-GEM7 gravity difference model.

In the second category, the estimated errors of the geopotential coefficients—the calibrated standard deviations—are used as the error model. These standard deviation values are obtained from the corresponding calibrated error covariance matrix obtained for each geopotential model (References 3, 4, and 5). However, it was demonstrated in References 6 and 7 that the use of GEM9 standard deviations as a lumped error model can be faulty, because of the anomalous global distribution of acceleration errors that is greater in the northern hemisphere with a singularity near zero degree longitude and 60 degrees latitude. Such anomalous distribution is not supported, however, by other evidence (References 3 and 8).

1.2 UNCORRELATED ERROR MODEL

The uncorrelated error modeling approach (UEMA) is generally used with the standard deviations models and assumes that each spherical harmonic coefficient can be treated as an independent error source. The orbital error caused by the geopotential error is then computed as the root sum square (RSS) of the independent error contributions from all the harmonic coefficients. This approach still requires a substantial amount of computational resources when compared with the LEMA because it requires evaluating one variational equation for each of the spherical harmonic coefficient error sources (Reference 2). For example, for the GEMT1 model with degree and order of 36, UEMA will require evaluating 1363 variational equations. Although some of the coefficients are known to be correlated (Reference 8), this approach may be reasonable (short of having to consider the correlations by including the entire covariance matrix).

It was demonstrated in Reference 6, using the GEM9 standard deviations model, that this approach produced more uniform global error distribution and more "realistic" orbital error distribution, and has, thus, been used previously in sequential error analyses performed for GSFC.

The study presented in this paper investigates the LEMA and UEMA in terms of global error distribution characteristics and reasonableness of error magnitudes predicted for a variety of spacecraft orbital scenarios. The reasonableness of a geopotential error model is assessed in terms of global error distribution characteristics and orbit error analysis results. The geopotential error models studied are listed in Table 1. The study results are presented in two parts.

In the first part, the global error distribution characteristics are analyzed for each of the geopotential models described in Table 1. In the second part of the study, the orbit determination

Table 1. Geopotential Error Models and Modeling Approaches Investigated in This Study

Geopotential Model	Corresponding Error Models		Approach
	Model	Size (Deg. Order)	
GEM 9	GEM9 Standard Deviations GEM9 Standard Deviations GEM9 - GEM7 Gravity Difference [a]	30, 30	LEMA UEMA LEMA
GEM T1	GEMT1 Standard Deviations GEMT1 Standard Deviations GEMT1 - Clone [b]	36, 36	LEMA UEMA LEMA
GEM T2	GEMT2 Standard Deviations GEMT2 Standard Deviations GEMT2 - Clone [b]	50, 50	LEMA UEMA LEMA

6130G(22)-16

Notes:

LEMA: Lumped error modeling approach
UEMA: Uncorrelated error modeling approach

a. GEM9 - GEM7 difference model is the geopotential error model currently used for operational error analysis support to represent the 3 σvalues of GEM9 force model error. This model is derived by taking the 135% of GEM9 - GEM7 differences up to degree and order of 21 to represent commission errors of the terms used in operational orbit determination and 100% of GEM9 coefficients from degree and order of 22 up to 30 to represent omission errors.

b. The clone models (References 9 and 10) are constructed such that the gravity errors computed using the difference between the original models (GEMT1 and GEMT2) and the respective GEMT1 and GEMT2 clone models give similar results obtained using the full calibrated error covariance matrices. A multiplication factor of 3 can be applied to represent 3σ error values.

errors resulting from the geopotential errors are assessed by performing linear error analysis using the Orbit Determination Error Analysis System (ODEAS) (Reference 2) for a variety of spacecraft mission scenarios. Specifically, analyses were performed for the Gamma Ray Observatory (GRO), the Cosmic Background Explorer (COBE), and the Ocean Topography Experiment (TOPEX) types of missions, primarily in a sequential Kalman filtering mode.

2. RESULTS

The results of this study are presented in two parts. Section 2.1 discusses the global distribution of geopotential acceleration errors for each of the error models listed in Table 1. Section 2.2 discusses the orbit determination errors resulting from geopotential errors predicted by different geopotential models and modeling approaches for GRO, COBE, and TOPEX spacecraft missions.

2.1 GLOBAL DISTRIBUTION OF GEOPOTENTIAL ACCELERATION ERRORS

Errors in the spherical harmonic coefficients will cause errors in computing the geopotential accelerations (forces) acting on an orbiting spacecraft. These acceleration errors vary as a function of geocentric latitude and longitude, and the error magnitude decreases with the increase in orbital height for a fixed latitude and longitude grid point in space. Figures 1

through 9 show the acceleration error magnitudes (1σ values) as a function of geocentric latitude and east longitude at an altitude of 200 kilometers above the surface of the Earth for different geopotential error models and modeling approaches. The acceleration errors shown are in the units of mgal (10^{-5} m/sec^2), rounded to the nearest integer.

For the LEMA, the acceleration errors at each of the latitude and longitude grid points are computed by algebraically summing the contributions from each of the sine and cosine harmonic coefficients at that particular location, using Equation (2).

$$\Delta \bar{a}_{LEMA} = \sum_{n=2}^{n_{max}} \sum_{m=0}^{n} \left(\frac{\partial \bar{a}}{\partial C_n^m} \Delta C_n^m + \frac{\partial \bar{a}}{\partial S_n^m} \Delta S_n^m \right) \tag{2}$$

where n_{max} represents maximum degree of the geopotential error model, and $\Delta \bar{a}_{LEMA}$ represents an instantaneous geopotential acceleration error a spacecraft would experience due to errors in the spherical harmonic coefficients C_n^m and S_n^m, which are represented by ΔC_n^m and ΔS_n^m in Equation (2). The acceleration error maps obtained using this modeling approach are shown in Figures 1 through 6. In orbit error analysis computation using the LEMA, the spacecraft position and velocity errors are obtained by integrating the effect of $\Delta \bar{a}_{LEMA}$ given by Equation (2) in one variational equation.

For the UEMA, the acceleration errors are obtained by computing the RSS of the contributions from each of the sine and cosine harmonic coefficients rather than summing them algebraically. This approach is shown mathematically in Equation (3) where Δa_{UEMA} represents the acceleration error magnitude obtained using the UEMA. The acceleration error maps obtained using this modeling approach are shown in Figures 7 through 9.

$$\Delta a_{UEMA} = \sqrt{\sum_{n=2}^{n_{max}} \sum_{m=0}^{n} \left(\left| \frac{\partial \bar{a}}{\partial C_n^m} \Delta C_n^m \right|^2 + \left| \frac{\partial \bar{a}}{\partial S_n^m} \Delta S_n^m \right|^2 \right)} \tag{3}$$

It should be noted that in orbit error analysis computation using the UEMA, the spacecraft position and velocity errors are obtained by integrating the individual vectors in the summation (i.e., $\frac{\partial \bar{a}}{\partial C_n^m} \Delta C_n^m$ and $\frac{\partial \bar{a}}{\partial S_n^m} \Delta S_n^m$) in separate variational equations and computing the RSS of all individual error contributions.

It is interesting to see from Figures 1 through 3 that all acceleration error maps obtained for the LEMA using the GEM9, GEMT1, and GEMT2 standard deviations models tend to show the same anomalous error distribution (i.e., a high concentration of large errors localized in a particular region around zero degree longitude in the northern hemisphere and the rest of the globe relatively error-free). The world map of gravity anomalies computed from GEM9 and GEM10 models (Reference 3), the gravity anomalies computed from GEM7 and GEM8, and the gravimetry data (Reference 8) do not support such anomalous distribution. This implies that the orbit determination errors predicted by using such error models will also be anomalous.

Figure 1.

<LONG>	0	20	40	60	80	100	120	140	160	180	200	220	240	260	280	300	320	340	360
90	16 16	16 16	16 16	16 15	15 15	14 14	14 13	13 13	13 12	12 12	12 12	12 13	13 13	13 14	14 14	15 15	15 16	16 16	16
80	25 25	25 23	21 18	16 13	11 9	7 5	5 4	4 4	4 5	5 6	6 6	7 8	9 10	11 13	15 17	19 20	21 22	23 25	
70	23 22	20 17	14 12	9 7	6 4	3 2	2 1	1 1	1 1	2 2	2 2	3 3	3 3	4 5	5 6	8 11	15 17	20 22	23
60	28 25	17 9	5 5	5 5	5 3	1 4	3 2	1 1	2 2	2 2	2 1	2 2	2 2	4 2	2 4	5 6	8 11	15 17	20 22 23
50	15 13	10 4	2 1	2 4	3 3	3 3	2 0	2 2	1 3	2 1	2 1	2 2	2 3	2 2	4 3	3 1	2 6	8 14	15
40	10 7	2 2	3 3	0 2	2 2	1 2	2 0	1 1	1 2	2 1	1 2	1 1	2 2	1 1	3 1	1 2	3 3	2 7	10
30	9 6	3 3	4 4	3 2	2 1	0 1	2 1	2 1	1 2	2 1	1 1	2 1	1 1	2 1	1 2	3 5	4 4	2 6	9
20	8 5	2 4	4 3	2 2	1 2	2 1	1 1	2 1	1 1	1 2	1 2	0 1	2 2	1 1	2 3	5 4	4 2	6 9	
10	7 3	2 3	3 2	1 1	1 2	1 1	1 2	2 1	1 1	1 1	2 1	2 0	1 2	2 1	2 3	4 4	1 5	8	
0	5 3	0 2	4 1	1 1	1 1	1 0	2 1	1 1	1 1	1 2	1 0	1 1	1 1	2 1	2 3	2 0	3 5		
-10	3 1	1 1	1 2	1 1	1 2	0 1	1 1	1 1	1 1	0 1	0 1	1 1	2 1	1 1	1 2	0 3	5		
-20	1 1	0 1	1 1	1 0	1 1	1 1	1 1	1 1	0 1	1 1	1 1	1 2	1 1	1 1	1 2	0 1	3		
-30	1 1	1 0	1 1	1 1	1 1	1 0	1 2	1 1	2 1	0 1	1 1	0 0	1 1	1 1	0 1	1 1	1		
-40	1 1	1 1	0 1	1 0	1 1	1 1	1 2	1 1	1 1	1 1	1 1	1 1	1 0	1 1	1 1	1 2	1		
-50	0 0	0 1	0 1	1 1	1 1	0 1	1 1	1 1	2 1	1 1	1 1	1 2	1 1	1 0	1 1	0 0	1 1		
-60	0 0	1 1	1 0	1 1	1 1	1 1	2 2	2 0	1 2	1 0	1 2	2 1	1 1	1 1	1 0	0 0	0 0		
-70	0 1	1 1	1 1	1 1	1 1	1 2	2 2	1 1	1 2	2 1	1 1	1 1	1 0	0 1	1 1	0 0			
-80	1 1	1 1	1 1	1 1	1 1	1 1	2 2	2 1	0 0	0 0	0 0	1 1	1 1	1 1	1 0	0 0	0 0		
-90	1 1	1 1	1 1	1 1	1 1	1 1	1 1	1 1	1 1	1 1	1 1	1 1	1 1	1 1	1 1	1 1	1		

Figure 1.   Gravitational Acceleration Errors (mgal) Based on the LEMA Using the GEM9 Standard Deviations Model

<LAT>

Figure 2.

<LONG>	0	20	40	60	80	100	120	140	160	180	200	220	240	260	280	300	320	340	360
90	19 19	19 19	19 19	18 18	17 16	16 15	14 14	13 13	12 12	12 12	12 12	12 13	13 14	14 15	16 16	17 18	18 19	19 19	
80	32 32	29 26	21 17	14 11	8 6	5 4	3 2	2 2	2 1	1 1	2 2	2 3	3 4	5 6	8 11	14 19	23 27	29 31	32
70	31 28	21 13	6 2	3 3	2 1	1 1	1 1	1 0	0 0	0 1	1 0	0 1	1 2	3 3	2 5	12 22	28 31		
60	22 17	7 2	4 3	3 2	2 1	1 0	1 0	1 0	0 0	0 0	0 1	1 0	2 1	2 2	3 4	2 7	18 22		
50	16 12	6 5	3 1	1 1	2 1	1 0	0 0	0 0	0 0	0 0	0 0	0 0	0 1	1 2	1 1	3 5	6 12	16	
40	15 10	5 2	1 2	2 2	1 1	0 0	0 0	0 0	0 0	0 0	0 0	0 1	1 1	2 2	3 1	2 5	10 15		
30	14 8	2 2	1 1	1 2	1 0	0 0	0 0	0 0	0 0	0 0	0 0	0 0	1 2	1 1	1 2	2 8	14		
20	13 7	0 3	1 2	1 1	2 1	1 0	0 0	0 0	0 1	1 0	0 0	0 0	0 1	1 1	2 1	3 0	7 13		
10	11 5	1 2	1 0	1 1	2 1	0 0	0 0	0 0	0 0	0 0	0 0	0 1	2 1	1 0	1 2	1 5	11		
0	7 3	1 2	0 1	1 0	2 0	0 0	0 0	0 0	0 0	0 0	1 0	2 0	1 1	0 0	2 1	3 7			
-10	2 1	0 1	0 0	0 0	1 1	1 0	0 0	0 0	1 0	0 0	0 0	1 1	1 0	0 0	1 0	1 2			
-20	0 0	0 0	0 0	0 1	1 0	0 0	0 0	0 1	0 1	0 1	1 1	1 0	0 0	0 0	0 0	0 0			
-30	0 0	0 0	0 0	0 0	1 1	0 0	0 0	1 1	1 0	0 0	1 1	0 0	0 0	0 0	0 0	0 0			
-40	0 0	0 0	0 0	0 0	1 1	1 0	0 1	0 1	0 1	0 1	0 0	1 1	0 0	0 0	0 0	0 0			
-50	0 0	0 0	0 0	0 0	0 1	1 1	0 0	1 1	0 1	0 1	1 1	1 1	0 0	0 0	0 0	0 0			
-60	0 0	0 0	0 0	0 0	0 1	0 1	1 1	1 1	1 0	0 1	0 1	1 1	0 0	0 0	0 0	0 0			
-70	0 0	0 0	0 0	0 0	1 1	1 0	0 1	1 1	0 1	1 0	0 1	1 0	0 0	0 0	0 0	0 0			
-80	0 0	0 0	1 1	1 1	1 1	1 1	1 1	1 1	1 1	1 1	1 1	1 1	0 0	0 0	0 0	0 0			
-90	1 1	1 1	1 1	1 1	1 1	1 1	1 1	1 1	1 1	1 1	1 1	1 1	1 1	1 1	1 1	1 1	1		

Figure 2.   Gravitational Acceleration Errors (mgal) Based on the LEMA Using the GEMT1 Standard Deviations Model

<LAT>

Figure 3.

<LONG>	0	20	40	60	80	100	120	140	160	180	200	220	240	260	280	300	320	340	360
90	26 27	27 27	26 26	25 24	23 22	21 20	19 18	17 17	16 15	15 15	15 15	16 16	17 18	18 19	20 21	22 23	24 24	25 26	26
80	30 29	26 21	17 14	11 8	5 4	3 2	2 2	2 1	1 1	1 1	1 1	1 2	3 4	5 6	8 11	15 19	22 25	28 30	
70	35 30	18 5	2 3	3 4	3 1	1 1	1 1	1 1	1 1	2 1	1 1	1 2	1 1	1 2	4 4	3 3	5 18	30 35	
60	21 13	5 1	5 4	2 2	1 2	1 1	1 1	1 1	0 1	1 1	0 1	1 1	1 3	1 2	0 4	5 0	5 12	21	
50	18 12	4 2	5 1	1 1	1 1	1 1	0 0	0 1	1 0	1 0	0 1	1 1	1 1	2 5	2 4	12 18			
40	13 5	4 2	3 1	1 1	1 1	1 1	0 0	0 1	1 1	1 0	0 0	1 1	1 1	1 1	1 3	2 4	5 13		
30	14 3	5 1	1 1	1 1	0 1	1 0	0 0	0 0	0 1	0 0	0 1	0 0	1 1	1 1	0 1	1 1	1 4	3 14	
20	13 4	3 1	1 1	1 1	1 1	0 0	0 0	0 0	0 0	0 0	0 0	0 0	0 1	1 2	1 3	4 13			
10	11 3	2 1	1 0	1 0	2 0	1 0	0 0	0 0	0 0	0 0	0 0	0 1	0 1	1 0	1 1	2 3	11		
0	6 2	1 1	1 0	1 0	0 0	0 1	0 0	0 0	0 0	0 1	0 0	0 0	0 1	0 1	1 1	1 6			
-10	2 0	1 0	0 0	0 0	0 0	1 0	0 0	0 1	0 1	1 0	0 0	0 1	1 1	0 0	0 0	0 2			
-20	0 0	0 0	0 0	0 0	1 0	0 1	0 0	0 1	1 0	0 0	1 1	1 0	0 0	0 0	0 0	2			
-30	0 0	0 0	0 0	0 0	1 1	0 0	1 0	0 1	1 0	0 1	0 0	1 0	0 0	0 0	0 0	0			
-40	0 0	0 0	0 0	0 0	1 0	0 0	0 1	0 0	1 0	0 1	1 0	0 0	0 0	0 0	0 0	0			
-50	0 0	0 0	0 0	0 0	0 0	1 1	1 0	0 0	0 0	1 1	1 1	0 0	0 0	0 0	0 0	0			
-60	0 0	0 0	0 0	0 0	0 0	1 0	1 1	0 0	0 1	1 1	1 0	0 0	0 1	1 0	0 0	0 0			
-70	0 0	0 0	0 0	0 0	0 1	1 1	0 0	0 0	0 0	0 0	1 0	1 1	0 0	0 0	0 0	0			
-80	0 0	0 0	0 1	1 1	1 1	1 1	1 1	1 1	0 0	0 1	0 0	0 0	0 0	0 0	0 0	0			
-90	1 1	1 1	1 1	1 1	1 1	1 1	1 1	1 1	1 1	1 0	1 1	1 1	1 1	1 1	1 1	1 1			

Figure 3.   Gravitational Acceleration Errors (mgal) Based on the LEMA Using the GEMT2 Standard Deviations Model

<LAT>
```
90  1 1 1 1 1 1 1 1 1 1 1 1 1 1 1 1 1 1 1 1 1 1 1 1 1 1 1 1 1 1 1 1 1 1 1 1 1
80  1 2 2 2 2 2 2 2 2 2 2 2 1 1 1 1 1 1 1 1 2 2 2 2 2 2 2 2 2 2 2 2 2 1 1 1 1
70  : 2 2 1 1 2 2 2 2 2 3 3 3 3 3 3 3 3 3 3 2 2 2 2 2 2 2 2 3 2 2 2 2 2 1 1 1 2
60  : 2 1 1 3 5 4 4 4 3 2 2 2 2 4 5 4 4 4 3 3 2 2 3 4 4 4 3 3 3 3 2 3 3 2 1 1 2
50  : 3 3 3 4 3 1 2 2 1 2 2 3 3 6 5 3 2 1 1 1 2 2 2 3 2 2 2 2 1 1 2 2 1 0 2
40  : 2 1 1 2 2 1 3 3 3 1 1 3 3 3 2 2 1 0 1 0 1 2 3 2 2 2 1 1 1 2 1 2 1 1 2
30  : 3 2 2 1 2 3 5 2 1 1 1 2 2 1 1 2 1 1 1 1 2 1 2 2 1 2 2 0 3 3 3 2 1 2
20  : 2 2 3 1 0 3 2 3 2 1 1 2 2 1 1 1 1 2 1 2 1 2 2 3 1 2 2 3 3 2 3 2 0 1 4 2 2
10  : 3 3 3 2 2 1 3 3 1 1 2 2 1 1 2 1 3 2 1 1 1 3 2 1 1 2 2 2 3 3 3 2 1
0   : 2 4 4 1 2 2 2 2 2 2 2 2 1 2 2 2 2 1 1 1 1 1 1 1 0 2 1 2 2 2 1
-10 : 4 4 2 1 1 2 1 2 2 2 1 1 1 2 2 1 3 2 1 1 2 2 2 1 1 1 2 1 2 1 2 2 3 3 4
-20 : 2 2 3 1 0 1 1 2 1 1 2 0 1 2 2 2 1 2 1 2 0 2 2 3 3 2 2 0 3 3 2 1 1 2 2
-30 : 2 1 2 2 1 1 1 1 1 1 0 1 1 1 1 2 1 3 2 1 2 1 1 1 1 1 1 1 1 1 2 3 3
-40 : 1 1 2 3 2 2 1 2 1 1 1 1 2 2 2 3 2 2 1 2 2 2 2 1 1 1 1 1 1 1 1 2 1
-50 : 2 1 1 1 2 3 3 3 2 2 2 4 4 4 3 2 1 1 2 2 1 1 1 1 3 4 4 4 3 2 2 2 3 2 2 3
-60 : 2 2 2 1 2 1 1 3 3 3 3 3 2 2 1 1 1 1 1 1 1 1 1 3 3 3 2 2 2 1 1 2 2 3 3
-70 : 2 2 2 3 3 2 2 2 2 2 3 3 3 3 3 2 2 3 2 2 2 2 2 1 1 1 1 1 1 2 2 2 2 2 2
-80 : 2 1 1 1 1 0 0 1 1 1 1 1 2 2 2 2 2 1 1 1 1 1 1 1 1 0 0 0 0 1 1 1 1 2 2 2
-90 : 1 1 1 1 1 1 1 1 1 1 1 1 1 1 1 1 1 1 1 1 1 1 1 1 1 1 1 1 1 1 1 1 1 1 1
```
<LONG>
0 20 40 60 80 100 120 140 160 180 200 220 240 260 280 300 320 340 360

Figure 4. Gravitational Acceleration Errors (mgal) Based on the LEMA Using the GEM9-GEM7 Difference Error Model

<LAT>
```
90  5 4 4 4 4 4 4 4 4 4 4 5 5 5 5 5 5 5 5 5 5 5 5 5 5 5 5 5 5 5 5 5 5 5 5 5
80  1 1 2 2 2 2 2 2 2 3 4 6 7 6 5 3 2 2 2 2 2 3 3 4 4 5 6 7 6 5 3 1 1 2 1
70  3 3 3 2 4 3 3 3 4 5 3 2 4 3 2 2 2 2 4 5 6 7 8 6 5 3 3 3 3 4 2 4 3 3 5 6
60  0 3 4 4 3 3 2 3 2 2 3 4 6 5 5 5 2 4 3 3 1 3 3 3 3 2 2 3 1 4 3 2 1 3 3 4 1
50  1 4 7 4 3 3 2 2 2 3 1 3 3 3 3 4 4 6 4 2 3 4 4 2 4 2 2 3 3 2 2 3 2 2 4
40  4 2 3 5 1 5 1 1 2 4 3 4 3 2 3 1 7 7 4 4 2 3 3 2 2 1 4 4 3 2 2 3 3 2 4 3
30  5 4 5 2 5 1 3 1 3 5 4 3 3 4 2 4 1 5 2 3 4 4 6 3 2 2 3 4 3 2 4 3 2 4 3
20  4 7 7 2 3 4 6 1 4 4 4 4 4 5 4 3 4 4 4 2 4 4 5 4 3 1 3 2 8 5 6 3 4 4 1
10  1 2 3 4 4 5 4 7 4 6 6 2 2 1 3 2 1 1 4 4 3 4 6 4 4 4 5 4 4 3 2 B 9 1 2 1 4 3
0   3 4 6 3 6 4 3 2 5 5 3 3 1 3 3 4 3 5 4 1 3 1 3 4 4 2 2 3 4 2 8 9 1 2 1 4 3
-10 3 9 4 3 4 5 3 6 5 3 1 3 3 4 3 5 4 1 3 1 3 2 6 3 2 3 6 4 4 7 5 3 3 8 4 3
-20 3 1 6 3 5 2 5 4 2 1 2 3 2 3 5 4 4 3 4 2 5 1 3 5 4 4 3 8 6 6 2 3 2 3 8 3
-30 3 2 1 4 4 5 4 2 4 3 1 1 3 3 2 6 5 4 2 2 2 4 1 4 3 1 2 5 6 6 5 3 3 4 3
-40 5 4 3 4 2 1 1 1 4 1 3 4 3 3 3 2 2 2 3 2 2 0 4 2 3 2 3 2 4 2 2 2 2 2 3 5
-50 3 7 4 1 1 1 1 2 5 2 1 2 0 2 1 3 4 3 3 2 4 6 3 3 4 4 2 3 3 4 4 3 3 2 2 3
-60 3 3 1 2 4 4 2 2 3 2 3 3 2 2 2 5 3 1 2 1 2 2 2 1 1 1 2 3 1 5 3 1 2 4 1 3 3
-70 5 4 4 3 2 2 3 3 4 3 2 2 3 4 3 3 3 4 3 4 3 3 7 8 5 4 4 4 4 3 4 4 4 5
-80 4 3 2 2 2 3 4 4 3 2 2 2 3 4 5 5 4 3 3 4 4 5 6 6 6 5 4 3 3 4 4 5 5 5 4 4 4
-90 2 2 2 2 2 2 2 3 3 3 3 3 3 3 3 3 3 3 3 3 3 3 3 2 2 2 2 2 1 1 1 1 1 1 2 2 2
```
<LONG>
0 20 40 60 80 100 120 140 160 180 200 220 240 260 280 300 320 340 360

Figure 5. Gravitational Acceleration Errors (mgal) Based on the LEMA Using the GEMT1-Clone Difference Error Model

<LAT>
```
90  3 3 3 2 2 2 2 2 2 2 2 2 2 2 2 2 2 2 2 3 3 3 3 3 3 3 3 3 3 3 3 3 3 3
80  1 1 3 4 4 4 4 5 4 4 5 6 6 5 5 5 5 4 3 2 3 4 4 4 4 5 6 5 4 4 4 4 2 1
70  2 1 2 3 2 4 2 3 2 1 4 4 4 4 3 2 3 3 4 2 2 1 2 2 2 3 3 3 3 3 2 3 4 2
60  0 1 1 3 3 3 3 1 2 2 2 3 3 2 2 1 2 2 1 2 4 2 3 3 3 3 2 2 0 2 1 2 1 2 1 5 3
50  3 4 4 2 1 2 2 2 1 2 5 4 3 2 5 3 2 2 3 2 3 4 2 4 3 4 4 2 3 4 3 3 3 3 4 2 3
40  3 3 2 2 1 2 4 3 4 3 3 2 1 2 3 2 5 2 3 3 4 2 4 3 4 4 2 3 4 3 3 3 3 4 2 1
30  1 3 3 2 2 4 4 1 4 2 1 2 3 5 2 2 4 4 3 3 3 5 0 3 1 3 5 3 4 4 9 7 3 2 4 3
20  2 3 4 2 4 3 3 3 3 2 2 3 1 4 5 2 1 4 3 2 2 3 4 4 9 7 3 2 4 3
10  5 5 3 2 4 2 4 3 3 2 1 6 2 3 4 6 2 7 5 3 3 4 2 3 4 5 6 3 5 3 9 5 8 4 5
0   6 1 3 3 3 2 4 1 4 3 6 6 3 4 2 2 5 3 1 2 5 2 5 5 2 2 5 4 3 2 5 5 6 4 8 4 5 6
-10 4 2 2 3 1 3 2 4 4 2 3 6 2 3 6 3 3 4 3 4 3 7 3 2 6 2 4 4 3 2 5 5 5 5 6 4
-20 3 2 2 4 2 2 4 5 2 2 8 2 4 4 3 4 2 4 4 4 6 2 5 2 3 4 5 5 3 1 3 3 3 3 3
-30 3 2 4 2 2 1 2 2 1 4 2 3 3 1 2 2 3 2 3 2 3 1 3 1 2 1 4 5 3 1 4 4 2 2 1 3
-40 1 1 5 2 3 2 4 2 1 2 2 2 1 1 1 1 2 2 2 2 2 1 3 2 2 1 3 5 2 1 2 2 2 1 1
-50 2 2 2 1 2 1 1 2 3 3 3 2 1 2 1 2 4 5 4 1 1 2 2 3 1 4 2 1 1 4 3 3 3 1 2
-60 3 3 1 1 2 2 1 1 4 2 3 5 4 2 4 4 4 2 1 1 1 1 4 4 2 4 3 1 1 2 2 2 2 3 4 4 3
-70 5 4 4 4 3 2 1 3 3 3 3 4 3 1 2 3 3 4 3 4 3 3 5 5 5 5 5 3 3 4 5 3 4 5
-80 2 2 2 4 5 5 5 5 3 3 3 4 4 5 6 6 5 4 3 3 4 4 5 5 5 2 4 5 5 4 4 2
-90 4 4 4 3 3 3 3 3 3 3 3 3 3 3 2 2 2 2 2 2 2 2 3 3 3 3 3 4 4 4 4 4 4 4
```
<LONG>
0 20 40 60 80 100 120 140 160 180 200 220 240 260 280 300 320 340 360

Figure 6. Gravitational Acceleration Errors (mgal) Based on the LEMA Using the GEMT2-Clone Difference Error Model

6130-15   235

Figure 7. Gravitational Acceleration Errors (mgal) Based on the UEMA Using the GEM9 Standard Deviations Model
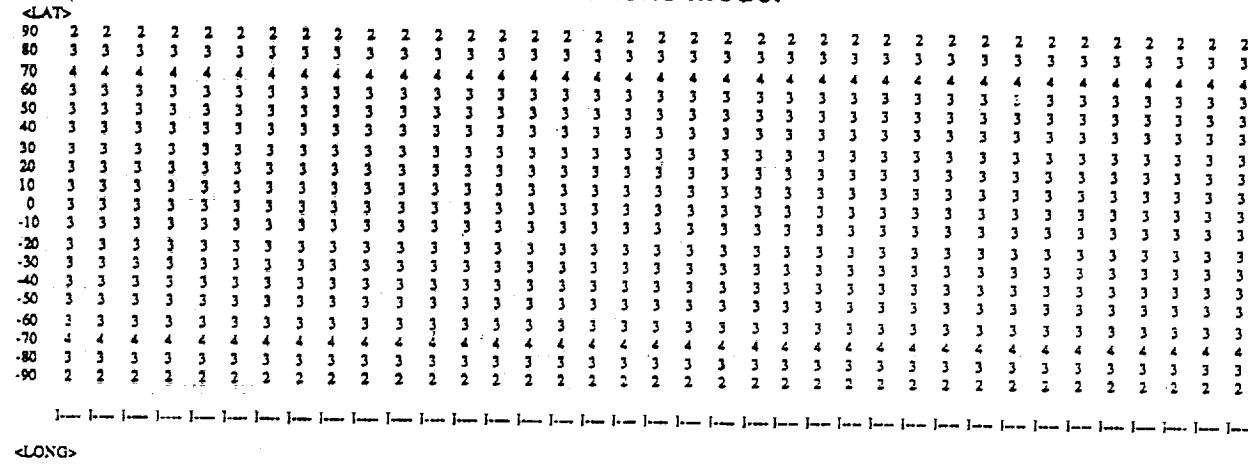
Figure 8. Gravitational Acceleration Errors (mgal) Based on the UEMA Using the GEMT1 Standard Deviations Model
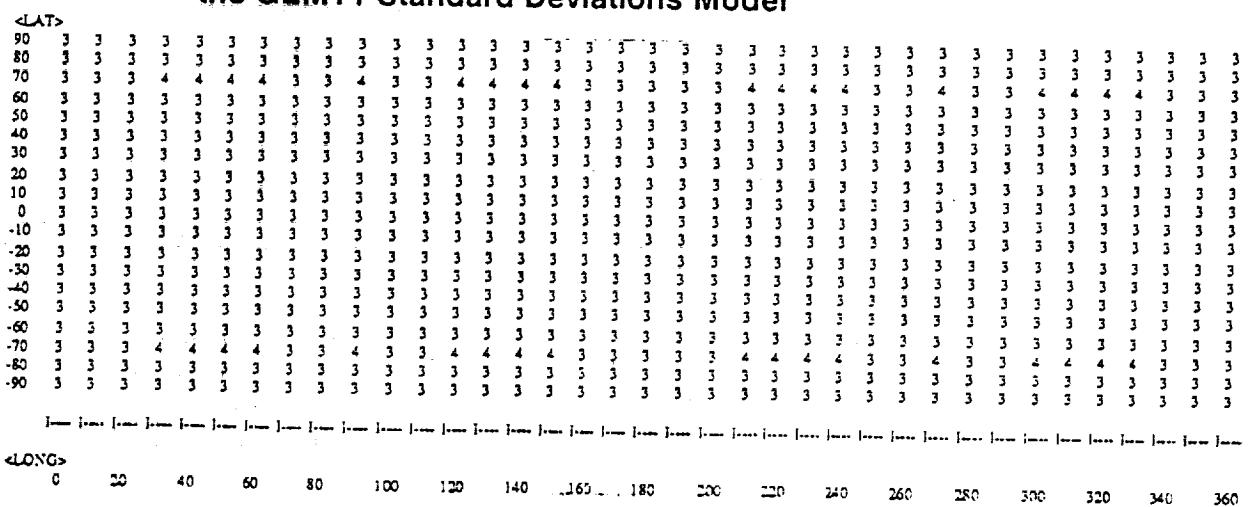
Figure 9. Gravitational Acceleration Errors (mgal) Based on the UEMA Using the GEMT2 Standard Deviations Model

On the other hand, the acceleration error distributions obtained for the UEMA seem to be too uniform and symmetric to be realistic. (See Figures 7 through 9.) Comparisons between GEM models and surface gravity measurement data (References 3 and 8) show that a more realistic error distribution may be somewhere between these two cases.

It is also interesting to see that the LEMA based on the gravity difference models (i.e., GEM9-GEM7, GEMT1-Clone, and GEMT2-Clone models) give rise to error maps showing random distributions in error magnitudes. (See Figures 4 through 6.) In the absence of the absolute standard, the gravity difference models appear to be more realistic in terms of global acceleration errors distribution.

2.2 ORBIT DETERMINATION ERRORS RESULTING FROM GEOPOTENTIAL MODELING ERRORS

To assess the orbit determination errors that result from the geopotential modeling errors, linear error analyses were performed using ODEAS for a variety of spacecraft missions with different altitudes and inclinations. Specifically, error analyses were performed for GRO, COBE, and TOPEX missions assuming an orbit determination mode using a sequential Kalman filter. Batch-weighted least-squares results are also shown for COBE spacecraft.

The orbital elements at epoch for GRO, COBE, and TOPEX, their respective spacecraft parameters, force models, and the integration parameters used in the study are shown in Table 2. Tracking simulations were performed for each spacecraft assuming a Tracking and Data Relay Satellite System (TDRSS) tracking scenario, whereby the user spacecraft (GRO, COBE, or TOPEX) is tracked for 2 days via TDRS-East (41 degrees west longitude) and TDRS-West (171 degrees west longitude) with tracking pass lengths of 20 minutes per user spacecraft revolution. Measurements include one range and one range rate every 10 seconds.

Error analyses were performed by estimating the orbital elements of the user spacecraft and the atmospheric drag scaling parameter. Because the primary interest of this study is in orbital errors resulting from the geopotential error sources, only the characteristics of geopotential errors on orbit determination accuracy are presented. The orbital errors presented below are based on 3σ errors.

Figures 10a through 10c illustrate the GRO (altitude: 450 km) spacecraft orbit determination errors resulting from the GEM9, GEMT1, and GEMT2 geopotential model errors, respectively. Figures 11 and 12 illustrate similar plots of orbit determination errors for COBE (altitude: 900 km) and TOPEX (altitude: 1340 km) spacecraft, respectively. Table 3 shows the root mean square (RMS) values, standard deviations, and maximum values of the orbital errors after the initial transient period (taken to be 6 hours past epoch).

The RMS and maximum errors resulting from a given geopotential error model are expected to decrease with increasing orbital altitudes from GRO to TOPEX. The orbital errors for a given spacecraft are also expected to decrease from GEM9 to the more refined models—GEMT1 and GEMT2. The observations made for each of the geopotential modeling approaches are summarized below.

1. *UEMA results using the standard deviations models* generally produce rather uniform error distributions at the expense of substantially higher computer processing times

Table 2.   Spacecraft Orbital Elements and Parameters

	GRO	COBE	TOPEX
EPOCH: (YYMMDD)	920201	921109	920901
(HHMMSS)	000000	000000	000000
ORBITAL ELEMENTS AT EPOCH			
Semi-major axis (km)	6828.15	7278.047	7718.756
Eccentricity	0.0001	0.0003238	0.00112783
Inclination (deg)	28.5	99.0296	63.14283
R. A. of ascending node (deg)	0.0	86.8450	0.0
Argument of perigee (deg)	0.0	94.9595	0.0
Mean anomaly (deg)	0.0	270.8221	0.0
Orbital Period (minutes)	93.59	102.99	112.48
SPACECRAFT PARAMETERS			
Drag coefficient (C_D)	2.2	2.3	2.3
Spacecraft area to mass (m^2/kg)	0.003347	0.006487	0.006487
Solar reflectivity (C_R)	1.5	1.3	1.3

FORCE MODELING

GEM9 30 X 30 for reference trajectory computation
Solar radiation pressure
Solid Earth tide
Atmospheric drag force using Harris-Priester density model
(Mean $F_{10.7}$ solar flux level = 175 X 10^{-22} watts/m^2/Hz)

ORBIT INTEGRATION

Integrator: Fourth-order Runge-Kutta Integrator
Step size: 60 seconds

TRACKING SCENARIO

20 min/user spacecraft orbit from TDRS-East or TDRS-West
Range noise = 3.0 m
Range-rate noise = 0.00282 m/sec
Date rate = 1 range and range rate per 10 seconds
For batch-weighted least-squares method, the data weights are set to be the same as for data noise

6130G(22)-17
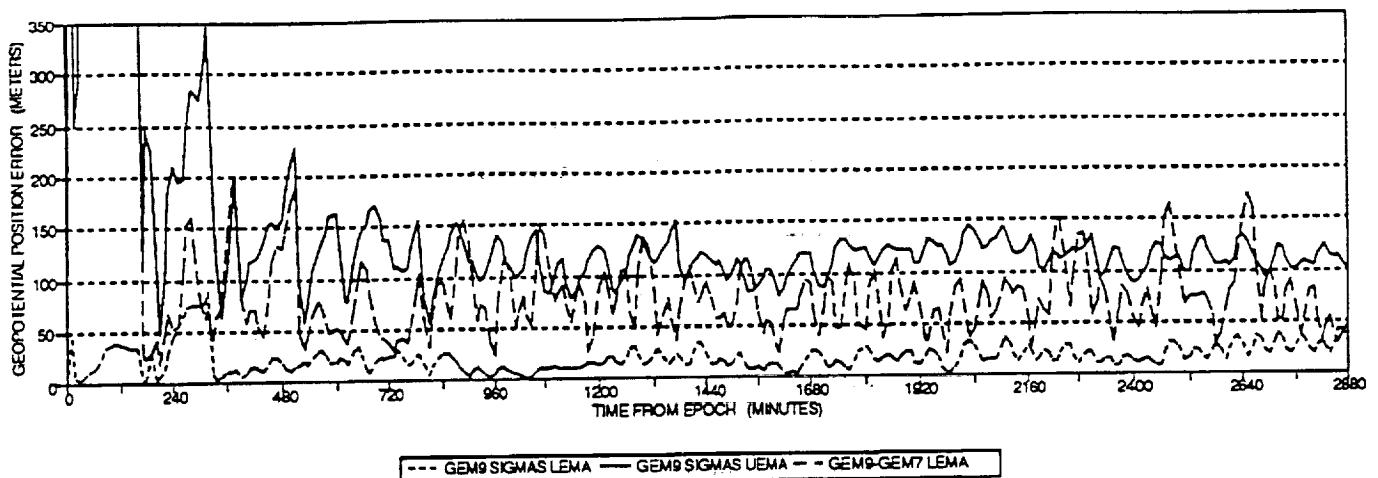
Figure 10a. GEM9 Geopotential Errors for GRO Processed in Sequential Mode
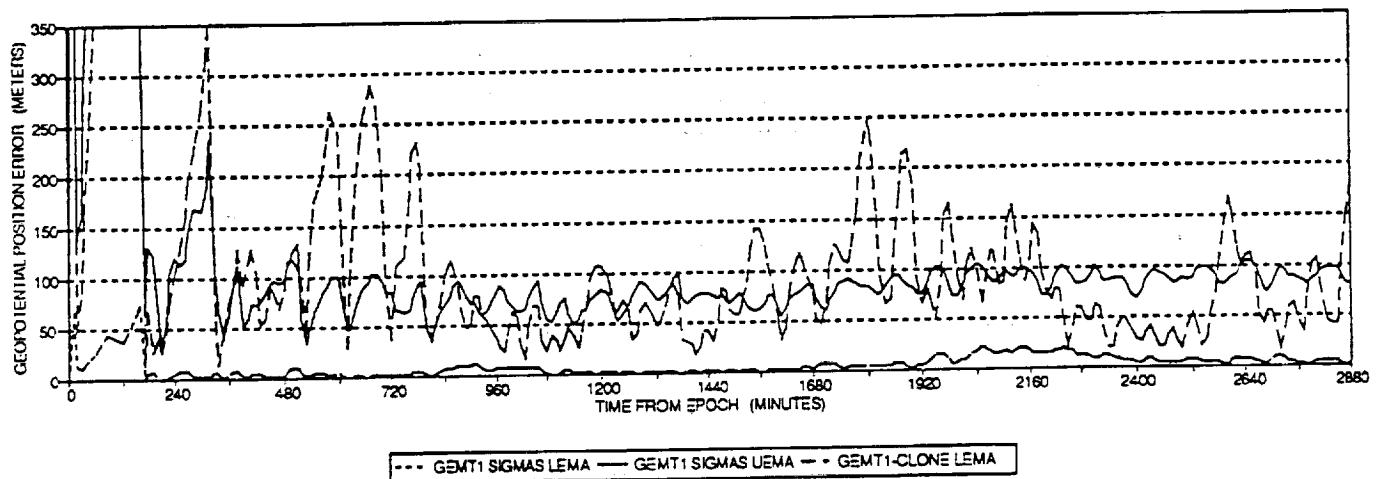
Figure 10b. GEMT1 Geopotential Errors for GRO Processed in Sequential Mode
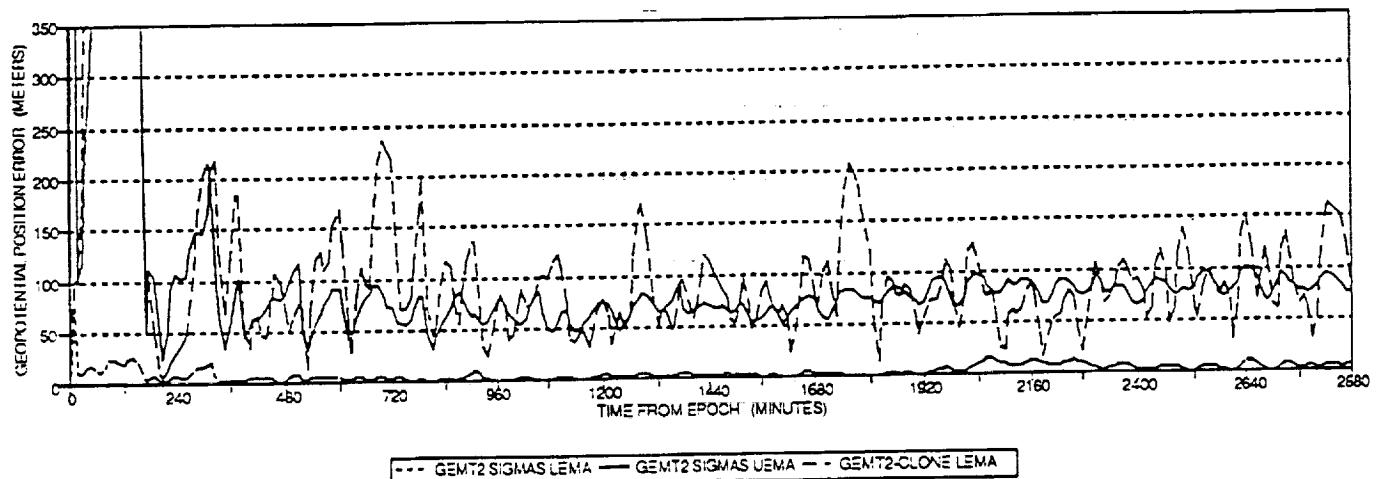
Figure 10c. GEMT2 Geopotential Errors for GRO Processed in Sequential Mode
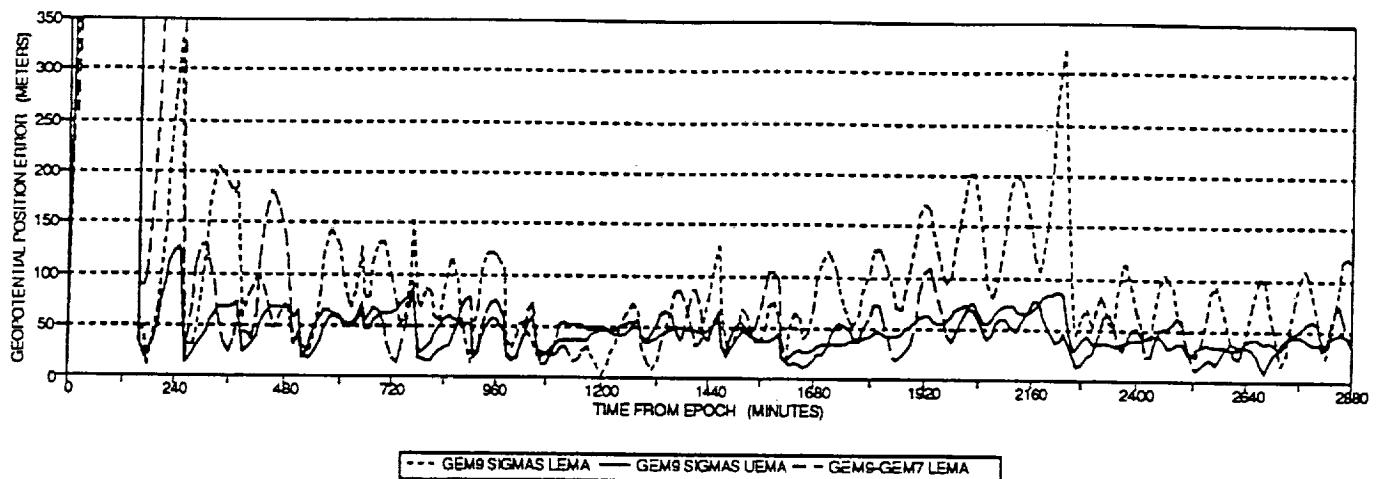
Figure 11a. GEM9 Geopotential Errors for COBE Processed in Sequential Mode
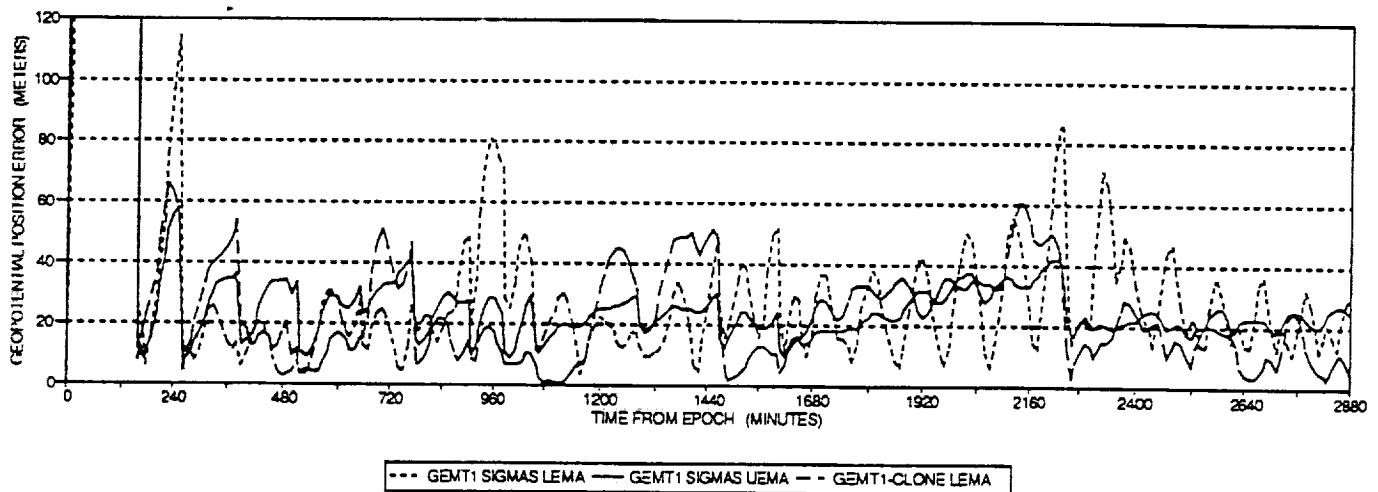
Figure 11b. GEMT1 Geopotential Errors for COBE Processed in Sequential Mode
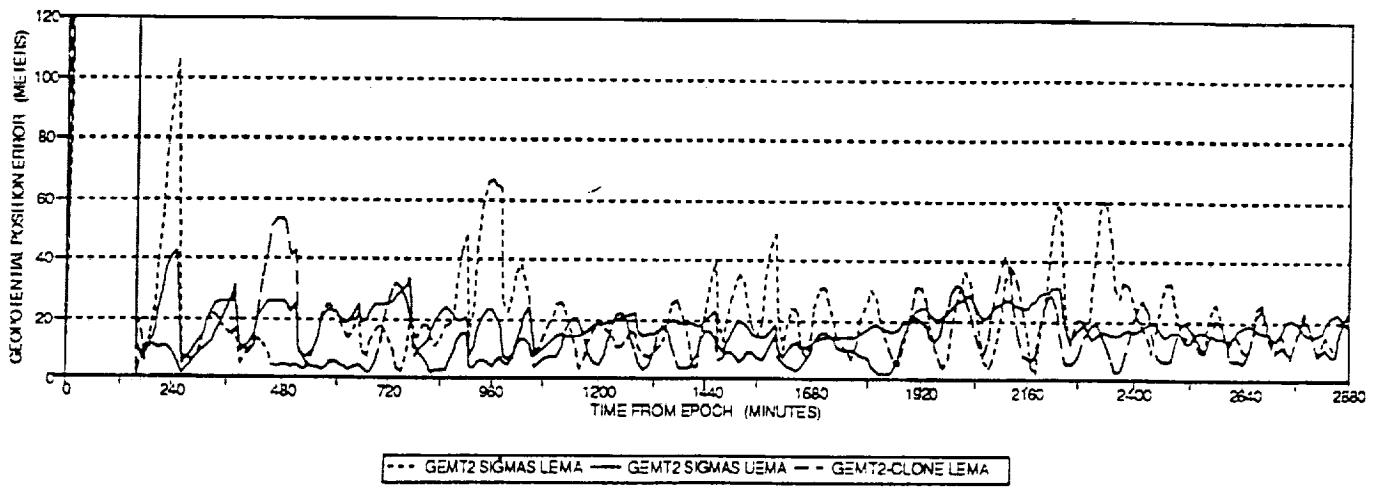
Figure 11c. GEMT2 Geopotential Errors for COBE Processed in Sequential Mode

6130-15

240
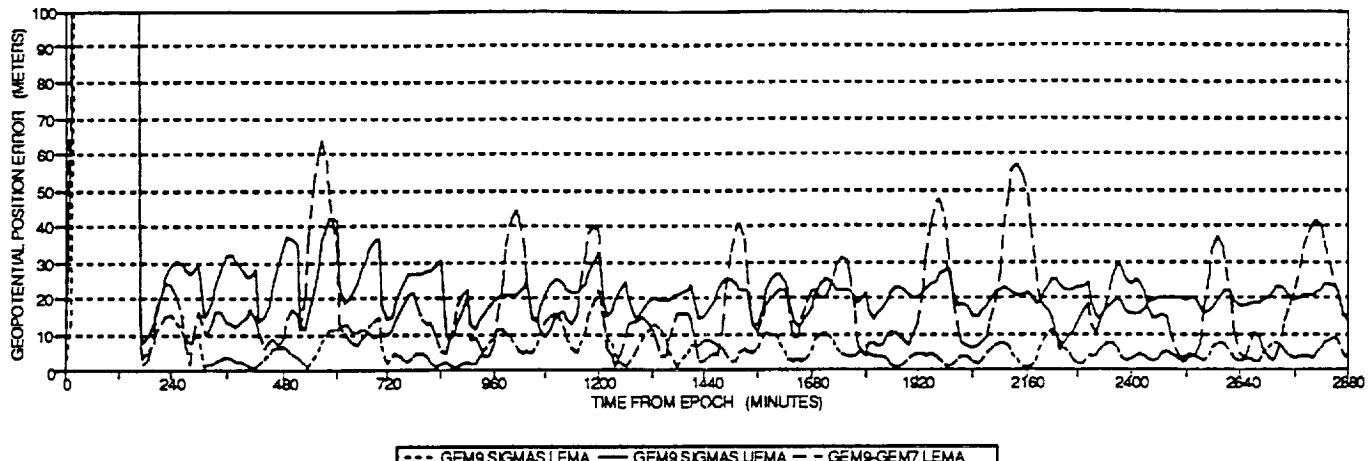
Figure 12a. GEM9 Geopotential Errors for TOPEX Processed in Sequential Mode
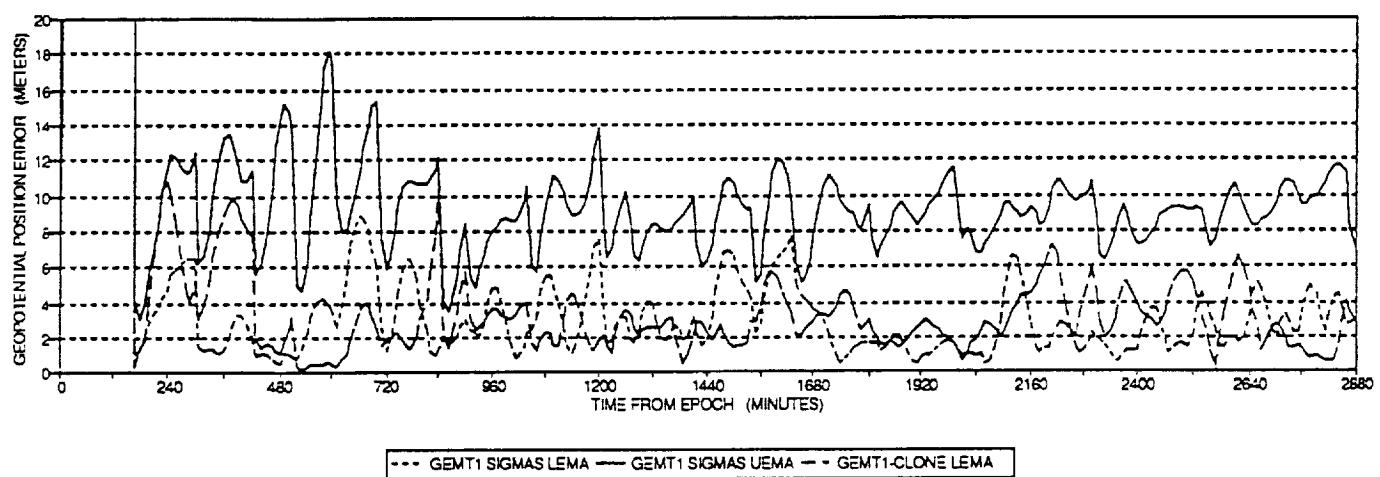
Figure 12b. GEMT1 Geopotential Errors for TOPEX Processed in Sequential Mode
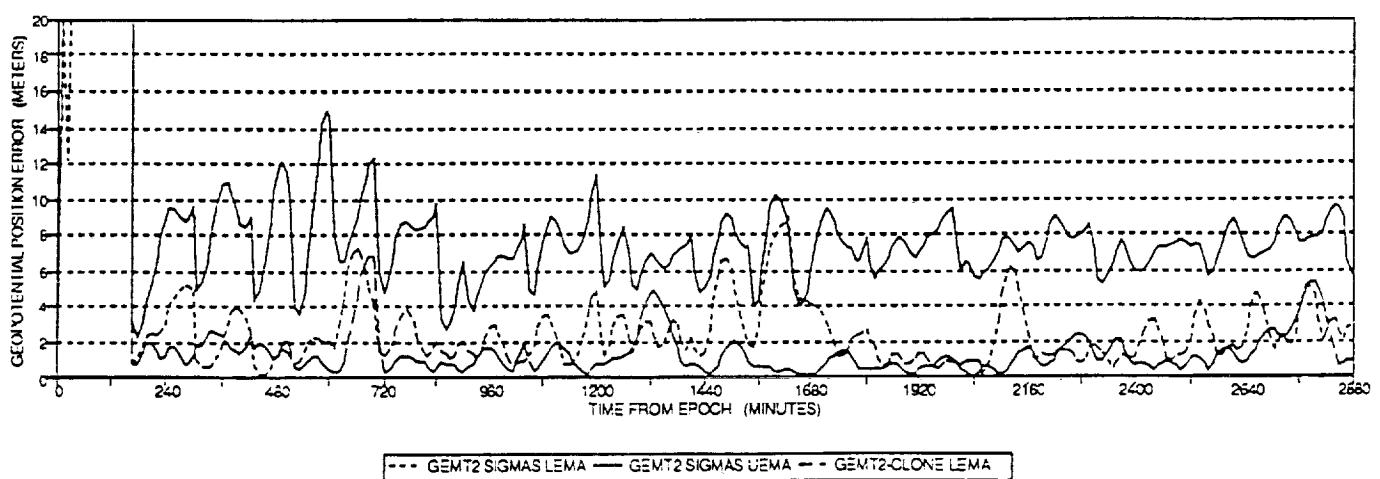
Figure 12c. GEMT2 Geopotential Errors for TOPEX Processed in Sequential Mode

	LEMA USING STANDARD DEVIATIONS			LEMA USING GRAVITY DIFFERENCES			UEMA USING STANDARD DEVIATIONS		
	GEM9	GEMT1	GEMT2	GEM9 [a]	GEMT1 [b]	GEMT2 [c]	GEM9	GEMT1	GEMT2
RMS									
GRO	20.462	8.578	5.693	85.155	105.188	96.495	119.717	83.700	76.112
COBE	96.004	30.581	23.799	56.067	26.588	16.786	48.529	25.288	19.211
TOPEX	6.598	3.463	3.027	22.459	3.527	1.813	22.111	9.500	7.689
Maximum									
GRO	42.344	23.146	15.784	200.430	288.670	235.400	227.350	135.420	117.960
COBE	323.620	86.041	66.670	181.480	60.767	53.962	85.404	43.749	34.032
TOPEX	22.229	8.848	9.052	63.587	10.399	6.866	42.564	18.198	15.028
Standard Deviation									
GRO	8.462	4.894	3.148	33.998	56.350	40.462	22.190	14.929	14.059
COBE	50.265	16.092	12.824	26.493	14.655	9.964	15.127	7.129	5.356
TOPEX	3.498	1.841	1.702	12.737	1.848	1.199	5.498	2.274	1.881

Units are in meters

Notes:

a. GEM9-GEM7 difference model is used to represent GEM9 errors
b. GEMT1-Clone difference model is used to represent GEMT1 errors
c. GEMT2-Clone difference model is used to represent GEMT2 errors

(generally requiring three to seven times as much central processing unit (CPU) time as the corresponding LEMA results). The uniformity is characterized by the relatively small standard deviation values when compared with the corresponding RMS values for all the spacecraft studied. Table 3 also indicates that the orbital errors predicted by the UEMA follow the expected trends.

2.   *LEMA results using standard deviations models* produce either large error spikes (as in the case of COBE) or relatively small errors (as in the case of GRO) when compared with the corresponding UEMA results. These results are expected because of the anomalous distributions of geopotential acceleration errors as illustrated in Figures 1 through 3. The effect of such distribution is that the orbital errors predicted for spacecraft with high orbital inclination, such as COBE (99 degrees), will result in large local error spikes. In contrast, the orbital errors predicted for spacecraft with lower orbital inclinations, such as GRO (28.5 degrees), can be unrealistically small. Such error characteristics are not supported by operational experience.

3.   *LEMA results using the gravity difference models* are found to exhibit different behaviors for different spacecraft orbital scenarios. From Table 3, it can be determined that the RMS and the maximum errors resulting from a given geopotential error model decrease, as expected, when going from a low-altitude orbit of GRO to a high-altitude orbit of TOPEX.

However, the orbital errors do not follow the expected decreasing trend from GEM9 to the more refined GEMT1 and GEMT2 error models for GRO, where the orbital errors resulting from the GEMT1-Clone and GEMT2-Clone error models are larger than those of GEM9-GEM7 error model. The error analysis results specific to each of the gravity difference models are summarized below:

- GEM9-GEM7 difference model produces reasonably close agreement with the GEM9 UEMA results for GRO and COBE spacecraft. For TOPEX spacecraft, while GEM9-GEM7 produces RMS orbital errors close to the UEMA results (Table 3), relatively large and spiky errors are observed in orbital error distributions. (See Figures 10a, 11a, and 12a.)

- GEMT1-Clone model produces results comparable with the GEMT1 UEMA results for COBE but produces comparatively higher errors in GRO and comparatively lower errors in TOPEX. (See Figures 10b, 11b, and 12b.)

- GEMT2-Clone model produces results comparable with the GEMT2 UEMA results for COBE but also produces comparatively higher errors in GRO and lower errors in TOPEX. (See Figures 10c, 11c, and 12c.)

To assess the reasonableness of the error magnitudes predicted by each error modeling approach, the orbital errors must be compared with independent results. Reference 5 provides independent error analysis results for TOPEX-type spacecraft for GEMT1 and GEMT2 models. These results were obtained using the first-order analytical perturbation theory of Kaula (Reference 11) and fully calibrated covariance matrices of GEMT1 and GEMT2 solutions, assuming a 10-day TOPEX arc.

Because such analyses do not account for the effect of imperfect tracking scenarios, the orbital errors thus obtained can be regarded as errors due entirely to the geopotential model under a perfect tracking condition. According to Reference 5, the projected orbital errors resulting from GEMT1 and GEMT2 model errors for a 10-day TOPEX arc are 1.9 and 0.9 meters (1σ), respectively. This translates to 5.7 and 2.7 meters (3σ) as shown in Table 4.

For comparison purposes, additional TOPEX error analysis was performed using the ODEAS sequential processing mode assuming a continuous tracking of TOPEX from TDRS-East and TDRS-West for 2 days using range and range-rate data. Continuous tracking was used to minimize the effect of imperfect tracking conditions on orbital errors. Table 4 lists the RMS orbital errors obtained after the initial transient period using different GEMT1 and GEMT2 error models.

The results indicate that, for TOPEX-type spacecraft, the projected orbital errors quoted in Reference 5 lie in between the UEMA and the LEMA results with UEMA results being on the high side.

Figures 13a through 13c show the batch-weighted least-squares orbit determination errors for COBE spacecraft resulting from GEM9, GEMT1, and GEMT2 error models, respectively. Error analysis results are presented assuming a 2-day definitive data for all cases. Again, it can be observed that the LEMA using standard deviations models produces very

Table 4. Comparison of TOPEX Orbital Errors (3σ values) Using Different Geopotential Error Modeling Approaches

Geopotential Model	Projected orbital errors for 10-day arc (meters) (Reference 5)	Steady-state RMS orbital errors for a 2-day continuous tracking (meters)	
		UEMA	LEMA[a]
GEMT1	5.7	7.4	3.2
GEMT2	2.7	6.1	1.3

6130G(22)-19

Notes:

a. GEMT1-Clone and GEMT2-Clone gravity difference models are used to represent geopotential errors due to GEMT1 and GEMT2 models, respectively.

large spikes in orbit errors. However, the LEMA using the gravity difference models produces results similar to the corresponding UEMA results. This was also found to be the case for COBE spacecraft in sequential processing mode. (See Figures 11a through 11c.)

Figures 14a through 14c compare COBE orbit determination errors processed in sequential Kalman filtering with batch-weighted least-squares modes using identical tracking schedules in both modes. As expected, the effects of local error spikes are less severe in the batch-weighted least-squares mode than in the sequential Kalman filtering mode, and the batch solutions agree with the corresponding sequential solutions at the end of the data arc.

3. CONCLUSIONS AND RECOMMENDATIONS

From the observation of geopotential acceleration error maps, two primary conclusions can be drawn.

1. The LEMA using standard deviations models produces an anomalous trend having a high concentration of large acceleration errors that are localized in a particular region around zero degree longitude in the northern hemisphere and the rest of the globe remains relatively error-free. Such an error distribution can give rise to spurious local error spikes for high-inclination spacecraft (such as COBE) and unrealistically small errors for low-inclination spacecraft (such as GRO). It can, therefore, be concluded that the standard deviations models should not be used in conjunction with the LEMA.

2. However, the UEMA using standard deviations models is found to produce uniform acceleration error bands symmetric in northern and southern hemispheres. This may, again, be unrealistic. On the other hand, the LEMA using gravity difference models gives error maps showing random distributions in error magnitudes. In the absence of the absolute
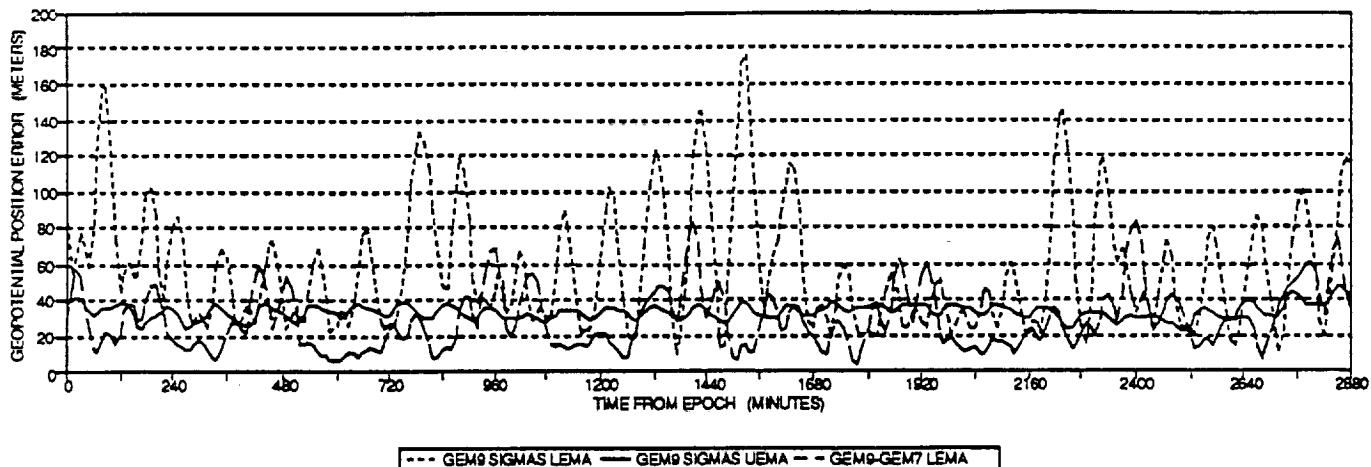
Figure 13a. GEM9 Geopotential Errors for COBE Processed in Batch Mode
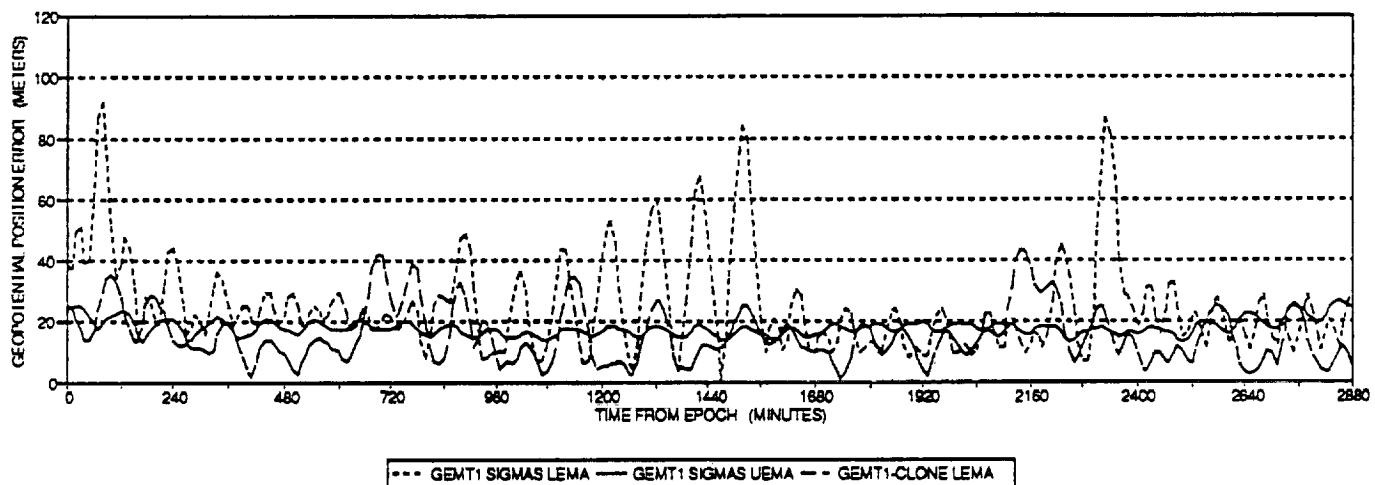

Figure 13b. GEMT1 Geopotential Errors for COBE Processed in Batch Mode
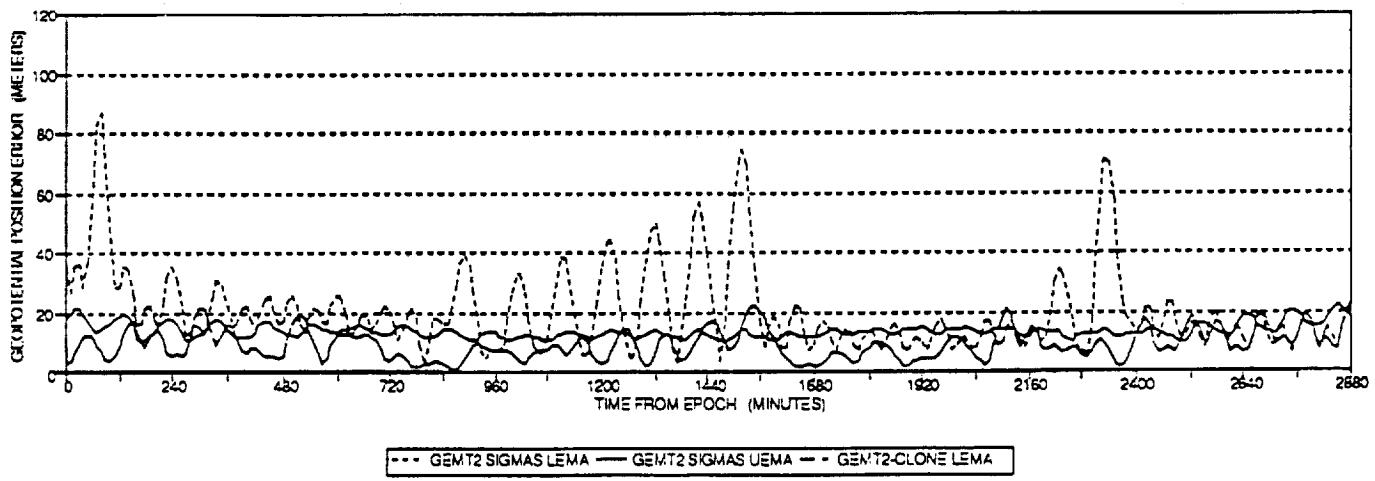
Figure 13c. GEMT2 Geopotential Errors for COBE Processed in Batch Mode

6130-15

245
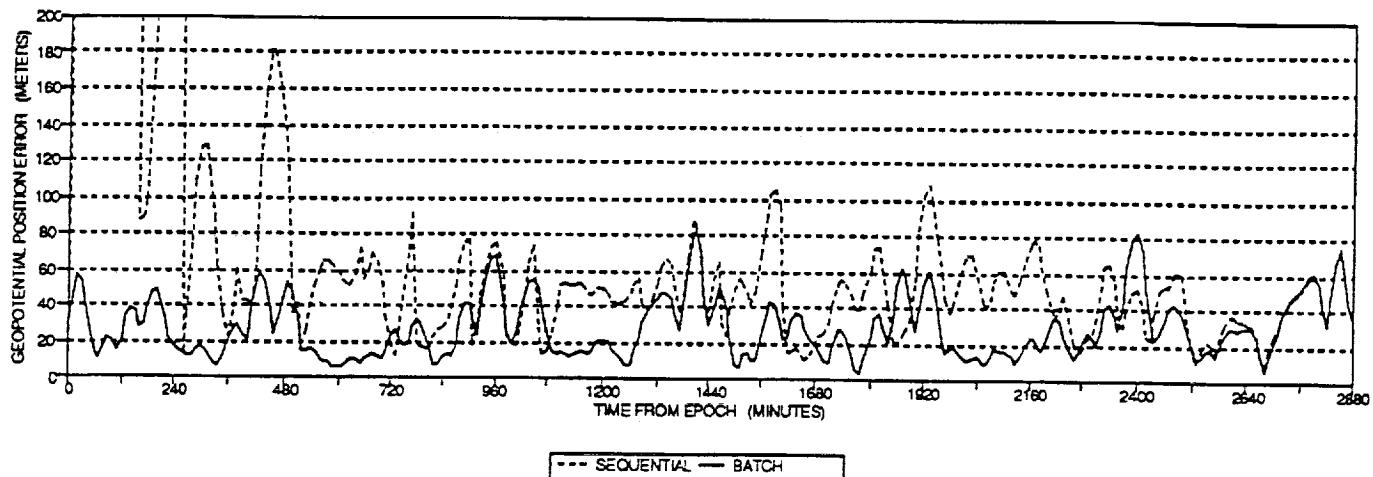
Figure 14a. Geopotential Errors for COBE Using GEM9-GEM7 Model
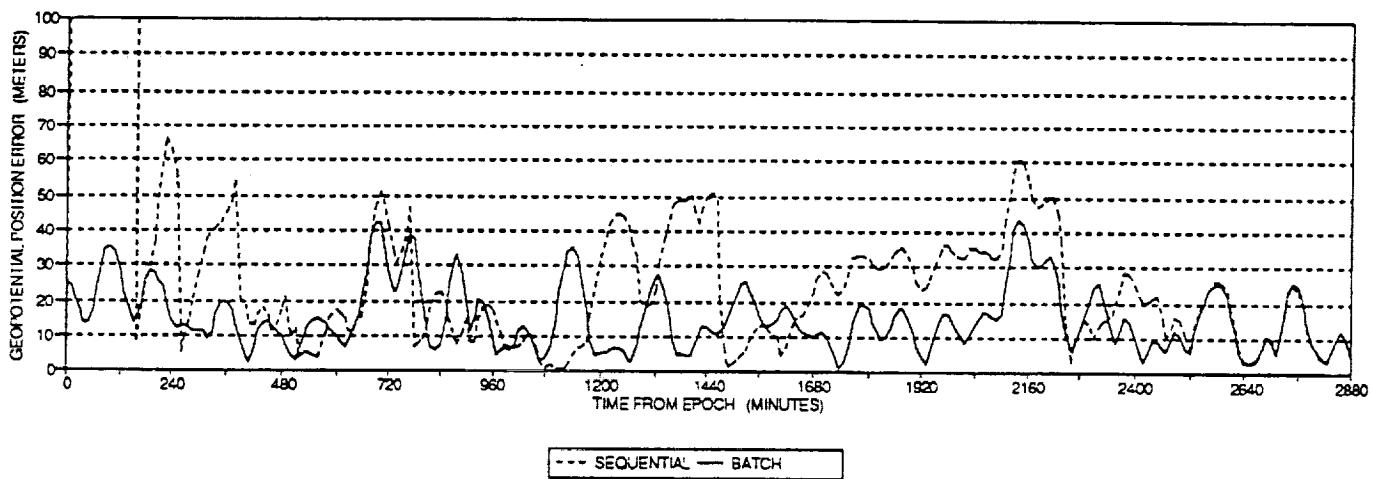
**Figure 14b. Geopotential Errors for COBE Using GEMT1-Clone Model**
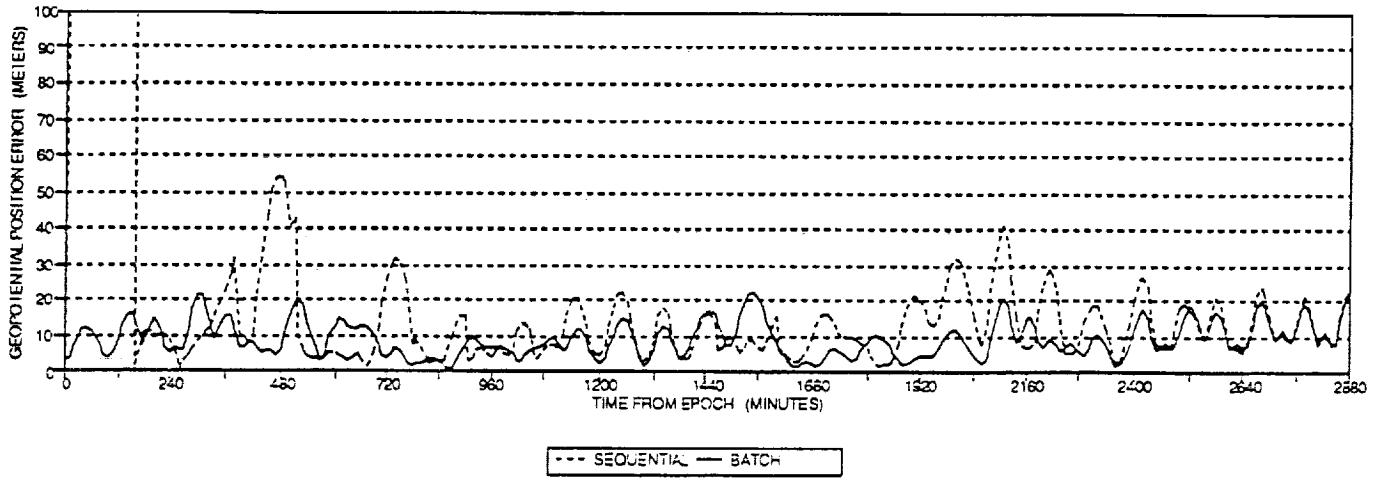
Figure 14c. Geopotential Errors for COBE Using GEMT2-Clone Model

6130-15

246

standard, the error characteristics shown in the gravity difference models appear to be the more reasonable representation of geopotential errors.

From the error analysis results, three additional conclusions can be drawn.

1.   The geopotential error models that are based on the UEMA generally produce fairly uniform error distributions usually free from unrealistic error spikes at the expense of substantially higher computer processing times (generally requiring three to seven times as much CPU as the LEMA). The uniformity is characterized by relatively small standard deviation values when compared with the corresponding RMS values. This was found to be the case in both sequential and batch processing modes. Also, the orbital errors predicted by this modeling approach generally follow the expected trends—meaning that, for a given geopotential error model, the RMS and the maximum orbital errors decrease with increasing orbital altitudes from GRO to TOPEX; and for a given spacecraft, the orbital errors decrease from GEM9 to the more refined models (GEMT1 and GEMT2).

2.   The difference error models in LEMA generally produce higher fluctuation in errors than the UEMA. This is characterized by relatively large standard deviation values when compared with the corresponding RMS values.

3.   Generally, the error characteristics produced by different geopotential error modeling approaches are not sensitive to orbit error estimation mode. For COBE spacecraft, the error signatures produced by the batch-weighted least-squares mode are similar to those of sequential Kalman filtering mode, except that the error magnitudes and the error fluctuations are smaller in batch mode. This is expected because of the data-smoothing effect realized in the batch estimation mode.

It is difficult to suggest a general error modeling approach that can be used for all spacecraft scenarios. As discussed earlier, if central processing unit (CPU) and computing resources are not of a concern, error analysis should be performed using the entire covariance matrix of spherical harmonic coefficients, to account correctly for the correlations that exist among these coefficients. In the absence of this, the UEMA may be a reasonable error modeling approach for most spacecraft scenarios because the orbital errors predicted by UEMA are mostly free from unrealistic error spikes and follow the expected trends as discussed earlier. The disadvantage of this approach is still the substantially higher CPU requirement over the LEMA for operational error analysis support.

The LEMA using difference models, while computationally efficient, is found to exhibit different characteristics for different spacecraft. GEM9-GEM7 seems to be a good error model to represent GEM9 modeling errors for GRO and COBE spacecraft, but it is not very reasonable for TOPEX because of some sporadic, large error spikes. GEMT1-Clone and GEMT2-Clone models seem to be good error models for representing GEMT1 and GEMT2 errors, respectively, for TOPEX and COBE spacecraft, but tend to produce large error spikes in GRO spacecraft.

As discussed previously, geopotential error models based on either the LEMA or the UEMA do not properly take into account the correlations that exist among the harmonic coefficients. If computer resources permit, future studies should include orbital error analyses using the

entire covariance matrix of spherical harmonic coefficients to take proper account of the correlations. This will also provide a reference point for calibrating other geopotential error modeling approaches. Future study should also include the development of an improved error modeling approach feasible for operational use. Such a modeling approach will be based on a certain combination of LEMA and UEMA with proper correlation information obtained from the calibrated error covariance. To augment the error analysis results, the authors also recommend performing sequential and batch orbit determination studies using real tracking data.

ACKNOWLEDGMENTS

REFERENCES

1. Martin, C. F., and Roy, N. A., "Error Model for the SAO Standard Earth," *The Uses of Artificial Satellite for Geodesy*, AGU Monograph 15, Washington, D.C., 1970

2. Goddard Space Flight Center, Flight Dynamics Division, FDD/554-90/029, *Orbit Determination Error Analysis System (ODEAS) Mathematical Specifications, Revision 1*, C. P. Yee and T. Lee, prepared by Computer Sciences Corporation, January 1990

3. Goddard Space Flight Center, X-921-77-246, *Gravity Model Improvement Using GEOS-3 (GEM 9 & 10)*, F. J. Lerch, S. M. Klosko, R. E. Laubscher, C. A. Wagner, September 1977

4. Goddard Space Flight Center, NASA TM-4019, *An Improved Model of the Earth's Gravitational Field: GEM-T1*, J. G. Marsh, et al., July 1987

5. Goddard Space Flight Center, NASA TM-10076, *The GEM-T2 Gravitational Model*, J. G. Marsh et al., October 1989

6. Stanford Telecommunications, Inc., STI/E-TR-25066, *Tracking and Data Acquisition System (TDAS) for the 1990's*, Volume VI, TDAS Navigation System Architecture, B. D. Elrod et al., May 1983

7. Computer Sciences Corporation, CSC/TM-53-6119, *Navigation Study for Low-Altitude Earth Satellite*, P. R. Pastor, B. T. Fang, and C. P. Yee, December 1985

8. Goddard Space Flight Center, X-921-76-187, *The Accuracy of Goddard Earth Models*, C. A. Wagner, June 1976

9. Private communications with F. Lerch (GSFC)

10. Memorandum from S. Klosko (ST Systems Corporation) to E. Christensen (Jet Propulsion Laboratory) dated November 7, 1990

11. W. M. Kaula, *Theory of Satellite Geodesy*, Balisdell Publishing Co.: Waltham, Mass., 1966